Contribution from the Institute for Physical Sciences and Technology and Department of Chemistry, University of Maryland, College Park, Maryland 20742, and Vakgroep Anorganische en Theoretische Chemie, Subfaculteit der Scheikunde, Vrije Universiteit, 1081 HV Amsterdam, The Netherlands

Valence Electron Momentum Distributions in $Cr(CO)_6$ from (e,2e) Spectroscopy and SCF-MO Calculations

D. J. CHORNAY,[†] M. A. COPLAN,[†] J. A. TOSSELL,*[‡] J. H. MOORE,[‡] E. J. BAERENDS,[§] and A. ROZENDAAL[§]

Received May 25, 1984

Electron momentum distributions, $\rho(q)$, have been measured for $Cr(CO)_6$ at eight different binding energies within the valence region by using (e,2e) spectroscopy and have been compared with orbital electron momentum distributions calculated from Hartree–Fock (HF) and Hartree–Fock–Slater (HFS) wave functions. Fourier transformation of $\rho(q)$ for the $2t_{2g}$ orbital gives the wave function autocorrelation function $B(r)$, which provides direct evidence for Cr 3d and CO 2π mixing. The measured change in $\rho(q)$ over the region of binding energies from 12.7 to 16.5 eV indicates that the $8a_{1g}$ orbital has a binding energy near 16.0 eV. The measured momentum distributions for the MO's derived mainly from the CO 4σ orbital (with binding energies around 18 eV) are in good agreement with calculations. The substantial mixing of CO 4σ and 5σ character in the $7a_{1g}$ orbital of this group obtained by HFS calculations is strongly supported by the measured $\rho(q)$. Momentum distributions measured for higher energy features at 20.6 and 23.8 eV support their assignment as shake-up satellites as previously suggested.

Introduction

$Cr(CO)_6$ is an important prototype organometallic compound that has been studied by a variety of experimental techniques, including visible–UV absorption spectroscopy,[1] IR–Raman spectroscopy,[2] X-ray diffraction,[3] photoemission spectroscopy,[4] X-ray emission spectroscopy,[5] and electron transmission spectroscopy.[6] It has also been the subject of numerous theoretical investigations in which Hückel-type,[7] Hartree–Fock,[8] Hartree–Fock–Slater,[9] and multiple-scattering $X\alpha$[10] methods were used.

The assignments of the lowest energy intense UV absorption bands have been established, and the major features of the photoemission spectrum are now qualitatively understood. Recent experimental[3] and theoretical studies[9,10b] have basically supported the simple qualitative model,[11] which emphasizes donation of CO 5σ orbital electron density to Cr and mixing of Cr 3d and CO 2π orbital character in the highest energy occupied MO, the $2t_{2g}$. Nonetheless, there is no direct experimental evidence on the distribution of electron density in the $2t_{2g}$ orbital alone. There also remain questions about the relative energies of the MO's that are mainly derived from CO 5σ and 1π orbitals, the degree of mixing of CO 5σ character into the orbital set generally associated with the CO 4σ orbital, the degree of delocalization of the CO 4σ cation states, and the assignment of two weak photoemission features at about 20 and 23 eV. In this paper, we present data bearing on each of these point using a relatively new experimental technique called binary coincidence electron-impact ionization, or (e,2e) spectroscopy.[12] This technique has recently been used to interpret the difference in basicity of NH_3 and CH_3NH_2.[13]

(e,2e) spectroscopy is based on an electron-impact ionization reaction. By measuring the momenta of the incident, scattered, and ejected electrons, one can determine the instantaneous momentum of the ejected electron from conservation considerations. By repeating the process many times, one can determine the distribution of these momentum values. The momentum distribution function is called the momentum density just as the position probability function is the electron density. To understand the data in terms of the conventional orbital model, one must either recast the models in the momentum representation or transform the data into the configuration space representation. We will use both of these routes in this paper.

From the point of view of quantum mechanics, the incident, scattered, and ejected electrons are waves that under the appropriate experimental conditions can be represented as plane waves. If the bound-state total wave function can be represented by a single configuration product of one-electron wave functions

$$\Psi = A\prod_i \psi_i \qquad (1)$$

then in the binary encounter approximation the (e,2e) cross section is

$$\sigma_{(e,2e)} = K|\langle e^{i\vec{q}\cdot\vec{r}}|\psi(\vec{r})\rangle|^2 \qquad (2)$$

where K is a constant and the term in angular brackets is the Fourier transform of the spatial wave function for the orrbital from which the ejected electron has been removed. The transform is equivalent to the momentum space wave function $\phi(\vec{q})$, and its square modulus is the momentum density $\rho(\vec{q})$. Therefore

$$\sigma_{(e,2e)} = K\,\rho(\vec{q}) \qquad (3)$$

If the energy resolution of the spectrometer is inadequate to completely separate closely spaced ionizations, then the (e,2e) cross section will represent a summation of contributions from the various cation states, weighted by Gaussian energy factors and occupation numbers. Since this situation is encountered for most binding energies in the spectrum of $Cr(CO)_6$, it will be discussed more fully under Results.

The position space wave function $\psi(\vec{r})$ and the momentum function $\phi(\vec{q})$ are equivalent representations. Thus, $\phi(\vec{q})$ and $\rho(\vec{q})$ have the same nodal and symmetry properties as $\psi(\vec{r})$ and $\rho(\vec{r})$. The momentum density of a totally symmetric orbital such as an atomic s orbital, a diatomic σ_g orbital, or a polyatomic a_{1g} orbital has a maximum at the origin in momentum space. The momentum density for an orbital that is not totally symmetric, such as a p, σ_u, or π orbital, has a maximum at some intermediate value of $\vec{q}$. Because of the Fourier transform relation between $\psi(\vec{r})$ and $\phi(\vec{q})$, an orbital that is diffuse in one space is compact in the other. Similarly, the amplitude of $\rho(\vec{q})$ at small values of $\vec{q}$ is related to the amplitude of $\rho(\vec{r})$ at large distances.[12]

[†] Institute for Physical Sciences and Technology, University of Maryland.
[‡] Department of Chemistry, University of Maryland.
[§] Vrije Universiteit.

(1) Gray, H. B.; Beach, N. A. *J. Am. Chem. Soc.* **1963**, *85*, 2922.
(2) Hawkins, N. S.; Mattraw, H. C.; Salod, W. W.; Carpenter, D. R. *J. Chem. Phys.* **1955**, *23*, 2422.
(3) Rees, B.; Mitschler, A. *J. Am. Chem. Soc.* **1976**, *98*, 7918.
(4) (a) Higginson, B. R.; Lloyd, D. R.; Burroughs, P.; Gibson, D. V.; Orchard, A. F. *J. Chem. Soc., Faraday Trans. 2* **1973**, *69*, 1659. (b) Rajoria, D. S.; Kovnat, L.; Plummer, E. W.; Salaneck, W. R. *Chem. Phys. Lett.* **1977**, *49*, 64.
(5) Kravtsova, E. A. *J. Struct. Chem. (Engl. Transl.)* **1982**, *23*, 697.
(6) Giordan, J. C.; Moore, J. H.; Tossell, J. A. *J. Am. Chem. Soc.* **1981**, *103*, 6632. Tossell, J. A.; Moore, J. ., Olthoff, J. K. *J. Am. Chem. Soc.* **1984**, *106*, 823.
(7) Elian, M.; Hoffmann, R. *Inorg. Chem.* **1975**, *14*, 1058.
(8) (a) Hillier, I. H.; Saunders, V. R. *Mol. Phys.* **1971**, *22*, 1025. (b) Vanquickenborne, L. G.; Verhulst, J. *J. Am. Chem. Soc.* **1983**, *105*, 1769.
(9) (a) Baerends, E. J.; Ros, P. *Mol. Phys.* **1975**, *30*, 1735. (b) Heijser, W.; Baerends, E. J.; Ros, P. *J. Mol. Struct.* **1980**, *63*, 109.
(10) (a) Johnson, J. B.; Klemperer, W. G. *J. Am. Chem. Soc.* **1977**, *99*, 7132. (b) Bursten, B. E.; Freier, D. G.; Fenske, R. F. *Inorg. Chem.* **1980**, *19*, 1810.
(11) Huheey, J. E. "Inorganic Chemistry: Principles of Structure and Reactivity", 3rd ed.; Harper and Row: Ne w York, 1983; p 429.
(12) Moore, J. .; Tossell, J. A.; Coplan, M. A. *Acc. Chem. Res.* **1982**, *15*, 192: McCarthy, I. E.; Weigold, E. *Phys. Rep.* **1976**, *27C*, 275.
(13) Tossell, J. A.; Lederman, S. M., Moore, J. H.; Coplan, M. A.; Chornay, D. J. *J. Am. Chem. Soc.* **1984**.

0020-1669/85/1324-0877$01.50/0 © 1985 American Chemical Society

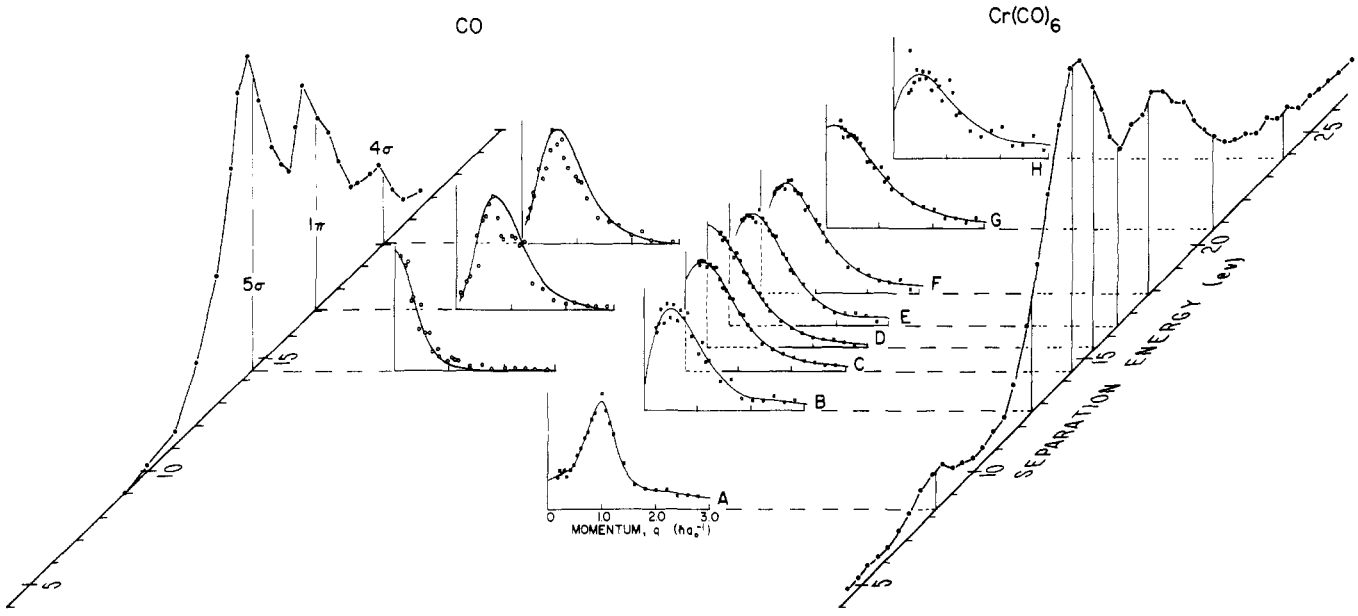

Figure 1. Separation energy spectra and experimental momentum distributions for CO and $Cr(CO)_6$.

A position space representation of the momentum density can be obtained by taking the Fourier transform of the momentum density.[14] The resulting function, $B(\vec{r})$,is the position space analogue of the well-known momentum space X-ray diffraction form factor, $F(q)$, which itself is the Fourier transform of the charge density. Since $\rho(\vec{q})$ and $B(\vec{r})$ contain the same information, it is legitimate to question the utility of $B(\vec{r})$. The usefulness of $B(\vec{r})$ is based on our bias toward thinking in position space rather than momentum space and the important practical point that the spherically averaged momentum density $\rho(q)$ can be measured directly in (e,2e) experiments, permitting one to obtain the spherically averaged $B(\vec{r})$ function, $B(r)$, from the data in a straightforward way. Weyrich et al.[15] have discussed in detail the $B(\vec{r})$ function for the investigation of the electronic structure of atoms and molecules. This $B(\vec{r})$ function can be calculated from the position space wave function $\psi(\vec{r})$ via the autocorrelation function

$$B(\vec{r}) = \int \psi(\vec{s})\, \psi(\vec{s} + \vec{r})\, d\vec{s} \qquad (4)$$

or, as we have mentioned, from momentum densities $\rho(\vec{q})$ via a Fourier transform

$$B(\vec{r}) = \int \rho(\vec{q})\, e^{-i\vec{q}\cdot\vec{r}}\, d\vec{q} \qquad (5)$$

Because the (e,2e) experiment measures the spherically averaged momentum density, $\rho(q)$, comparisons between theory and experiment will be restricted to discussions of the spherically averaged function $B(r)$. It is also useful to consider the difference between $B(r)$ functions for two orbitals i and j

$$\Delta B_{ij}(r) = B_i(r) - B_j(r)$$

The calculation of $\Delta B_{ij}(r)$ from the theoretical wave functions is facilitated by the following approximation, which is correct to second order in the orbital differences:

$$\Delta B_{ij}(\vec{r}) \approx \int [\bar{\psi}(\vec{s})\, \Delta\psi(\vec{r} + \vec{s}) + \bar{\psi}(\vec{r} + \vec{s})\, \Delta\psi(\vec{s})]\, d\vec{s} \qquad (6)$$

where

$$\bar{\psi}(\vec{s}) = \tfrac{1}{2}[\psi_i(\vec{s}) + \psi_j(\vec{s})] \qquad \Delta\psi(\vec{s}) = \psi_i(\vec{s}) - \psi_j(\vec{s}) \qquad (7)$$

Experimental Section

The instrument has been described previously.[12] $Cr(CO)_6$ was obtained commercially from Strem Chemical Co. and was used out of the bottle. To obtain sufficient gas density in the collision region of the spectrometer, the $Cr(CO)_6$ sample was maintained at 40–50 °C during the course of the experiment. The sample was always under vacuum and shielded from ambient light to eliminate photodecomposition. The incident electron energy was 800 eV. The cross sections obtained are, within the plane wave impulse approximation, proportional to momentum distributions $\rho(q)$ for the individual orbitals undergoing ionization.

Results

In Figure 1 we give a binding energy spectrum for $Cr(CO)_6$ obtained by summing over 25 values of momentums in the region from 0 to 3 $\hbar a_0^{-1}$, where $\hbar a_0^{-1}$ is the momentum of an electron in the ground state of H. Our spectrometer function is approximately Gaussian[16] with full width at half-maximum of about 2.0 eV—thus our energy resolution is intermediate between that typical for X-ray and UV photoemission spectra. The momentum resolution is 0.1 $\hbar a_0^{-1}$. We have acquired momentum distributions by measuring (e,2e) cross sections at binding energies of 8.4, 12.7, 14.5, 15.5, 16.4, 17.6, 20.6, and 23.8 eV, corresponding to the labels A–H in Figure 1. The measured momentum densities at these binding energies are shown in Figure 1. Results for CO are also included. Spherically averaged orbital momentum distributions have been calculated from a Hartree–Fock–Slater (HFS) wave function similar to that previously reported[9a] (see Appendix for details) and are shown in Figure 2. Using the program GAMESS,[18] we have also calculated $\rho(q)$ values from a HF type wave function obtained with a basis set that was minimal for all functions except Cr 3d, C 2p, and O 2p, for which split-valence representations were employed.[17] The calculated HF total energy at a Cr–C distance of 1.92 Å was −1708.3061 Hartrees, intermediate between those of ref 8a (−1702.6129 hartrees) and 8b (−1719.4277 hartrees).

Only for peak A can we associate the experimental $\rho(q)$ with a single orbital, the $2t_{2g}$. For the other energies there are significant contributions from several MO's. We therefore represent the theoretical momentum density at momentum q and energy E as

$$\sum_k n_k\, \rho_k(q)\, \exp\{-0.693[(E - E_k)/HW]^2\} \qquad (8)$$

where n_k is the occupation number of orbital k, $\rho(q)$ its momentum distribution, E_k its (assumed) binding energy, and HW the

(14) Benesch, R.; Singh, S. R.; Smith, V. H., Jr. *Chem. Phys. Lett.* **1971**, *10*, 151.
(15) Weyrich, W.; Pattison, P.; Williams, B. G. *Chem. Phys.* **1979**, *41*, 271.
(16) Migdall, J. N.; Coplan, M. A.; Hench, D. S.; Moore, J. A.; Tossell, J. A.; Smith, V. H., Jr.; Liu, J. W. *Chem. Phys.* **1981**, *57*, 141.
(17) (a) Rappe, A. K.; Smedley, T. A.; Goddard, W. A., III. *J. Phys. Chem.* **1981**, *85*, 2606. (b) Ditchfield, R.; Hehre, W. J.; Pople, J. A. *J. Chem. Phys.* **1971**, *54*, 724.
(18) Dupuis, M.; Spangler, D.; Wendowski, J. National Resource Computational Chemistry Software Catalog, Vol. 1, Program No. QG01.

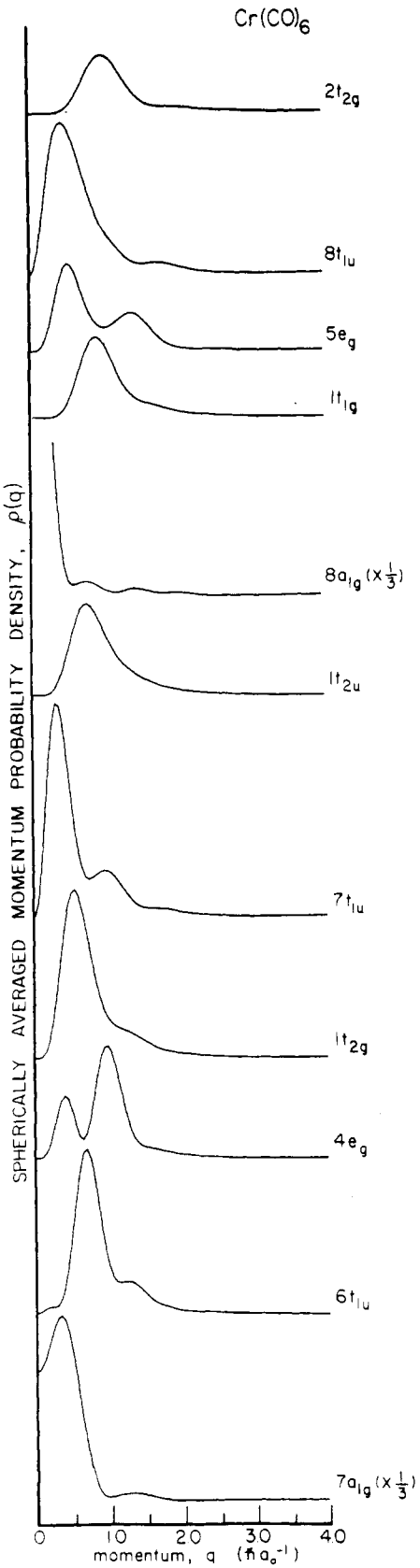

Figure 2. Orbital momentum distributions for $Cr(CO)_6$ from HFS calculations in order of calculated binding energies with smallest at top.

half-width at half-maximum of the spectrometer function. Thus, the quality of fit of the experimental and theoretical $\rho(q)$ at a given E depends upon the accuracy of both the orbital $\rho(q)$ and the orbital binding energies.

We have used the experimental binding energies as reported by Higginson et al.[4a] The assignment that these authors made of specific orbital ionizations to the experimental peaks did not agree with the ordering of orbital ionization energies obtained in HFS calculations by Baerends and Ros.[9a] We will consider both the Higginson (H) and the Baerends and Ros (BR) assignments. The two assignments are given in Table I, together with the calculated[9a] IP's, which deviate by 0.5–1.0 eV from experiment. The two resultant syntheses at points B, C, D, and F are shown in Figure 3. The synthesized result (using either set of BE's) at point A is virtually identical with that for the $2t_{2g}$ orbital alone, shown in Figure 4. We note that there is one important difference between the assignments of ref 4a (H) and 9a (BR). The $8a_{1g}$ orbital is more stable in the H assignment, leading to the highest BE in the CO 5σ, 1π band, instead of being in the middle, as in the BR assignment. However, larger basis set HFS calculations[28] give the $8a_{1g}$ orbital on the high BE edge of the CO 5σ, 1π band.

HFS calculations in which localization of the cation hole is allowed for ionization from the CO 4σ (and 3σ) type orbitals are in better agreement with experiment than the delocalized-hole calculations.[9a] This raises the possibility that the assignments (in both ref 4a and 9a) of the $4e_{1g}$ and $6t_{1u}$ orbitals to the 17.8-eV PES peak and the $7a_{1g}$ orbital to the 19.7-eV peak may be incorrect. Unfortunately, the CI calculation necessary to determine the $^2A_{1g}$, $^2T_{1u}$, and ^2E_g states of the $Cr(CO)_6^+$ ion from the localized 4σ hole determinantal wave functions has not been done. However, our experimental results strongly suggest that all the above states of the ion occur near 17.8 eV and that the 19.7 eV peak is a satellite. The synthesized spectra in Figure 3 all assume BE's of 17.8 eV for $4e_{1g}$, $6t_{1u}$, and $7a_{1g}$ orbitals. The necessity of this choice will be explained below.

Table I. Assumed Binding Energies and Orbital Assignments for $Cr(CO)_6$

		binding energies, eV		
		exptl		
orbital	type	H[a]	BR[b]	calcd BR
$2t_{2g}$	Cr 3d, CO 2π	8.4	8.4	8.9
$8t_{1u}$	CO 5σ	13.4	13.4	12.9
$5e_g$	CO 5σ	14.8[c]	14.2	13.9
$1t_{1g}$	CO 1π	14.2	14.4	14.6
$8a_{1g}$	CO 5σ	16.2	14.8[d]	14.7
$1t_{2u}$	CO 1π	14.4	15.1	14.8
$7t_{1u}$	CO 1π	15.1	15.6	15.0
$1t_{2g}$	CO 1π	15.6	16.2	15.2
$4e_g$	CO 4σ			
$6t_{1u}$	CO 4σ	17.8	17.8	18.3[e]
$7a_{1g}$	CO 4σ	19.7	19.7	

[a] Experimental BE's assigned according to Higginson et al.[4a] [b] Experimental BE's assigned according to Baerends and Ros.[9a] [c] $5e_g$ taken as middle of region 14.4–15.1 eV. [d] $8a_{1g}$ taken as middle of region 14.4–15.1 eV. [e] Symmetry-unrestricted calculation on localized cationic state.

Discussion

Before discussing the experimental momentum densities, we note that the relative heights of the peaks in the binding energy spectrum also contain qualitative information on $\rho(q)$. These heights are proportional to the sum of the 25 momentum values sampled by the spectrometer. However, for each orbital i there is the requirement that $\int \rho_i(q)\, q^2\, dq = n_i$, where n_i is the number of electrons in orbital i. If orbital i has its momentum density maximum at small q and orbital j has its maximum at large q (assuming $n_i = n_j$), the maximum value of $\rho(q)$ for i must be larger than that for j because of the q^2 weighing factor in the normalization integral. Thus, the very small height of peak A, associated with the 6 electrons in the $2t_{2g}$ orbital, indicates that the $2t_{2g}$ momentum distribution has its maximum at large q. In general, orbitals with large average momentums will generate weak features in an (e,2e) binding energy spectrum of this type where a wide range of momentum values are sampled and summed. Similar reasoning accounts for the difficulties in studying core states by this technique.

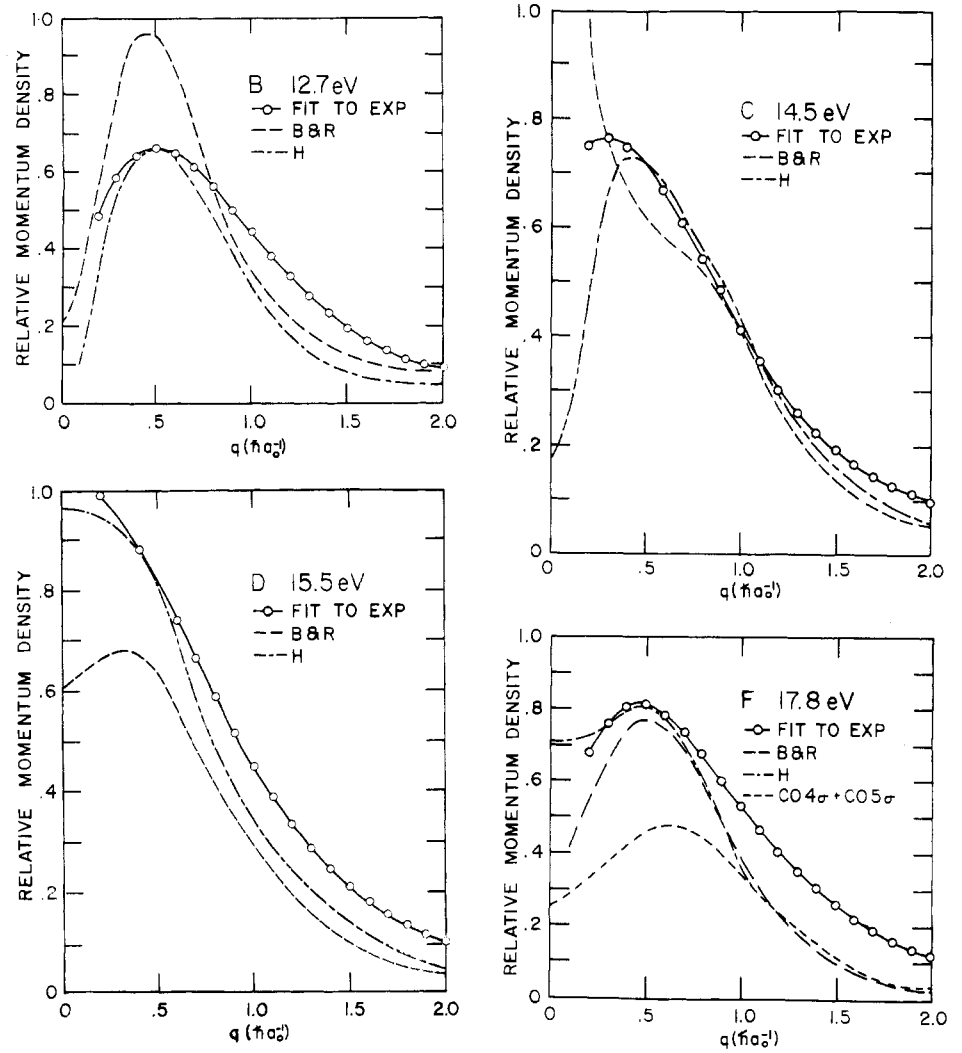

Figure 3. Comparison of experimental momentum distributions with those synthesized for HFS orbital momentum distributions at energies B, C, D, and F.

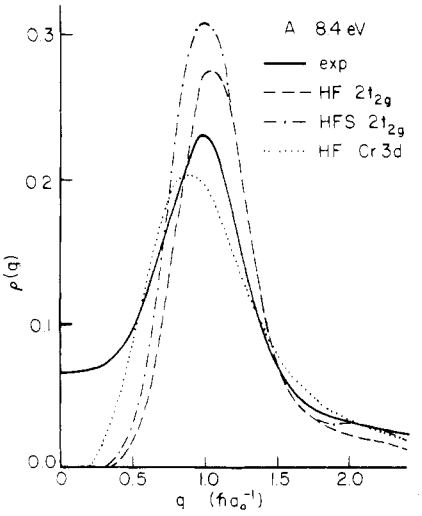

Figure 4. $\rho(q)$ from calculation and experiment for $2t_{2g}$ orbital.

For the $2t_{2g}$ orbital, the experimental $\rho(q)$ (peak A) is compared in Figure 4 with that from HF and HFS calculations on $Cr(CO)_6$ and with a HF calculation on thee $3d^6$ state of the free Cr atom.[17a] The molecular calculations reproduce the position of the $\rho(q)$ maximum quite well but are far below the experiment at both low and high q. The high experimental values of $\rho(q)$ in the region beyond 1.6 $\hbar a_0^{-1}$ may arise partly from failure of the plane wave impulse approximation as has been shown to occur in helium at high momentum.[19] The discrepancy at low q, although rather small when the radial momentum distribution $\rho(q)q^2$ is considered, is nonetheless real. To determine whether an increase in the Cr–C bond length could account for the difference between experiment and theory at small values of q, a HF calculation on O_h $Cr(CO)_6$ with a Cr–C distance 0.14 Å larger than that in the neutral compound (the distance in $Cr(CO)_6^+$ according to the PES analysis of Hubbard and Lichtenberger[20]) was performed. The result was a $\rho(q)$ almost indistinguishable from that for the neutral-molecule geometry in the low-q region.

For binding energies between 12.7 and 16.4 eV there is only one totally symmetric orbital, the $8a_{1g}$. The position of this orbital can be estimated by an inspection of momentum densities at low values of q within this region, assuming for the moment a single $8a_{1g}$ feature uncomplicated by correlation or vibrational effects. Since the momentum distribution at D is most like that of the $8a_{1g}$ orbital, this orbital must lie close to 15.5 eV.

We will now look in detail at peaks B, C, D, and F (neglecting E, which corresponds to a minimum in cross section). Experimental and calculated $\rho(q)$ plots for B, shown in Figure 3, are in qualitative agreement with a good correspondence in the position of the maximum although the experimental $\rho(q)$ is broader than that calculated and does not appear to go to zero at the origin. For peaks C and D somewhat better agreement with experiment

(19) (a) Dixon, A. J. McCarthy, I. E.; Noble, C. J.; Weigold, E. *Phys. Rev. A* **1978**, *17*, 597. (b) Leung, K. T.; Brion, C. E. *Chem. Phys.* **1983**, *82*, 87.

(20) Hubbard, J. L.; Lichtenberger, D. L. *J. Am. Chem. Soc.* **1982**, *104*, 2132.

is found by using the Higginson et al. assignment.[4a] In particular, $\rho(q)$ for D has its maximum at $q = 0$ for this assignment, in agreement with experiment. Agreement with experiment can be further improved by shifting the $8a_{1g}$ BE (assumed as 16.2 eV in the assignment) even closer to the position of D (15.5 eV). Calculated and experimental $\rho(q)$'s are also in reasonable agreement for peak F with the ref 4a assignment giving slightly better agreement due to a larger contribution for the nearby $8a_{1g}$ orbital. For this peak the value of $\rho(q)$ near the origin is dominated by the $7a_{1g}$ contribution, since the $8a_{1g}$ orbital is far away in energy and the $4e_g$ and $6t_{1u}$ orbitals have nodes at the origin. If the $7a_{1g}$ orbital were entirely CO 4σ in character, its momentum density near $q = 0$ would be very low, as for the CO 4σ orbital in Figure 1. Instead, peak F shows fairly high momentum density near the origin. Population analysis of the $7a_{1g}$ orbital[29] indicates somewhat unexpectedly that it has about 50% contribution from the CO 5σ orbital, which has a maximum at $q = 0$. Synthesis of peak F by summing the contributions of 11 CO 4σ-like electrons and 1 CO 5σ-like electron indeed gives a reasonable position for the $\rho(q)$ maximum and significant density at $q = 0$. In order to quantitatively reproduce the F distribution, however, we must consider the full MO result for the $7a_{1g}$ orbital (incorporating some Cr 4s character) and the contribution of the nearby $8a_{1g}$ orbital. The large value of $\rho(q)$ near $q = 0$ can only be reproduced in the synthesis if the $7a_{1g}$ BE is quite near 17.8 eV. This argues quite strongly for an assignment of the $7a_{1g}$ orbital to this peak rather than to the one at 19.7 eV. In addition, assignment of the $7a_{1g}$ ionization to the peak at 20.6 eV would give a synthesized momentum distribution with a maximum around 0.3 $\hbar a_0^{-1}$ (like that for the $7a_{1g}$ orbital) rather than the "s-like" momentum distribution observed at peak G and too low an intensity for peak F. Conversely, assignment of $7a_{1g}$ to the 17.8-eV peak and the $4e_g$ and $6t_{1u}$ orbitals to the 20.6-eV peak gives a maximum at too low a value of q for peak F and the wrong qualitative shape for peak G.

Thus, the shapes and intensities of peaks F and G are best explained by assuming that F corresponds to $4e_g$, $6t_{1u}$, and $7a_{1g}$ ionizations and G to a satellite. Inspection of $\rho(q)$ for G indeed shows it to closely resemble that of D. The $\rho(q)$ distribution for a satellite will generally resemble that of its parent.[12] Therefore, G is probably a satellite of orbitals near D. Similarly, H has a distribution much like that of F, suggesting that it is a satellite of the CO 4σ levels. The G–D and H–F separations are 5.1 and 6.0 eV, respectively, close to the satellite energies for O 1s and C 1s ionization observed in many metal carbonyls. Rajoria et al.[4b] have suggested that all of these satellites are involved with Cr 3d $\rightarrow$ CO 2π excitation. Recent HF–CI calculations[21] basically support this assignment although the calculated satellite energies are considerably larger than experiment.

Before leaving our overall discussion of peaks A–H, we shall consider some further effects that may explain the discrepancies observed between experiment and calculation at very small and very large q for peaks A and B. First, we have employed an independent electron model for $Cr(CO)_6$ ionization except for our identification of G and H as satellites. Full HF–CI or Green's function calculations of photoionization energies have not been reported for $Cr(CO)_6$, but approximate SCF many-body calculations[22] and small basis set–small CI GMO calculations[23] indicate that correlation effects in the upper valence region (8.4–16.5 eV) are small and that the Hartree–Fock ground-state configuration is by far the leading configuration (97%). Thus, it seems doubtful that such effects will be very important here. Nonetheless, since Cr 3d $\rightarrow$ CO 2π type satellites apparently exist for Cr 2p, O 1s, C 1s, and some valence region ionizations, it seems probable that the $2t_{2g}$ peak (A) has a similar satellite around 13–14 eV, which may contribute to the momentum density of B at low q. We have

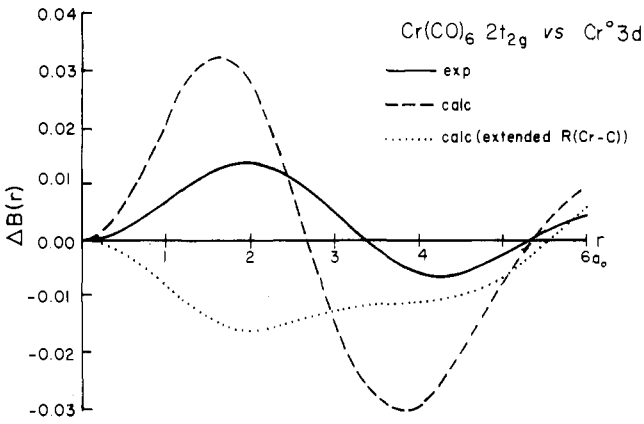

Figure 5. $B(r)_{2t_{2g}} - B(r)_{Cr\,3d}$ from HF calculation and experiment.

also ignored vibrational effects, except for our calculation of the $2t_{2g}$ orbital $\rho(q)$ at an enlarged Cr–C distance. The mean amplitude of vibration for the Cr–C bond is, however, quite large[24] (about 0.06 Å), and variation of R(Cr–C) and R(C–O) may affect momentum densities and binding energies. Our HF calculations indicate that generally $\rho(q)$ changes little even for orbitals strongly involved in bonding such as $2t_{2g}$ but that binding energies may be more strongly affected. Our calculations indicate that increasing R(Cr–C) by 0.14 Å destabilizes the $2t_{2g}$, $5e_g$, and $8a_{1g}$ orbitals by 0.9, 0.8, and 0.6 eV, respectively. Thus, a proper vibrational averaging might change the contributions of these orbitals due to their close spacing. The basis sets used are also of only modest size. In particular, no polarization functions ($l \geq 2$) are used on C and O. Wave functions near the Hartree–Fock limit have been found necessary to quantitatively describe the orbital $\rho(q)$ for CO while even Hartree–Fock-limit wave functions give a poor description of the π^* orbitals of NO and O_2.[25]

At present, we believe that the discrepancies between experiment and theory at high q (1.6 $\hbar a_0^{-1}$) arise mainly from distorted wave effects,[19] while those at small q are probably related to molecular vibrations. Excitation of degenerate vibrations gives average geometries that do not possess the full point-group symmetry. If the cation produced by orbital ionization is stabilized by a similar distortion, the appropriate geometry for evaluation of $\rho(q)$ will be intermediate between the symmetric ground-state geometry and the distorted cation geometry. Thus, orbitals with no a_1 character in the neutral molecule may show a_1 character, with finite $\rho(q)$ at $q = 0$, in the (e,2e) data, as previously observed for cyclopropane.[26] However, for $Cr(CO)_6$ there is not evidence for significant distortion of the cation formed by $2t_{2g}$ orbital ionization.

Having examined the general nature of $\rho(q)$ for peaks A–H, we can now address the question of Cr 3d–CO 2π bonding in the $2t_{2g}$ orbital. From $\rho(q)$ for peak A we can gain semiquantitative information on the position space distribution of electrons in the $2t_{2g}$ orbital, using the $B(r)$ approach. We first take the Fourier transform of the calculated and experimental $\rho(q)$'s to obtain $B(r)$ functions and then take differences of these $B(r)$ functions. Since distorted wave effects and experimental uncertainties in $\rho(q)$ are certainly significant for $q \geq 2.0$ $\hbar a_0^{-1}$, we integrate only from 0 to 2.4 $\hbar a_0^{-1}$. For this integration range, we find that $B(0)$, which is an overlap integral and must therefore be equal to unity when integrated over all space, has a value of about 0.6. The discrepancy between the experimental $2t_{2g}$ $\rho(q)$ at small q has almost no effect upon $\Delta B(r)$ since the $\rho(q)\,q^2$ contribution to the integral from this region is small. Conversely, the q^2 factor may lead to a larger discrepancy at large q.

In Figure 5 we give the $\Delta B(r)$ functions obtained by subtracting $B(r)$ calculated for the free Cr atom (in a d^6 configuration) from

(21) Hall, M. B.; Sherwood, D. E., Jr. *Inorg. Chem.* **1979**, *18*, 2323. Ford, P. C.; Hillier, I. H.; Pope, S. A.; Guest, M. F. *Chem. Phys. Lett.* **1983**, *102*, 555.
(22) Saddei, D.; Freund, H.; Hohlneicher, G. *Chem. Phys.* **1981**, *55*, 339.
(23) Sherwood, D. E., Jr.; Hall, M. B. *Inorg. Chem.* **1983**, *22*, 93.
(24) Jones, L. H.; McDowell, R. S.; Goldblatt, M. *Inorg. Chem.* **1969**, *8*, 2349.
(25) Tossell, J. A.; Moore, J. H.; Coplan, M. A.; Stefani, G.; Camilloni, R. *J. Am. Chem. Soc.* **1982**, *104*, 7416.
(26) Tossell, J. A.; Moore, J. H.; Coplan, M. A. *Chem. Phys. Lett.* **1979**, *67*, 356.

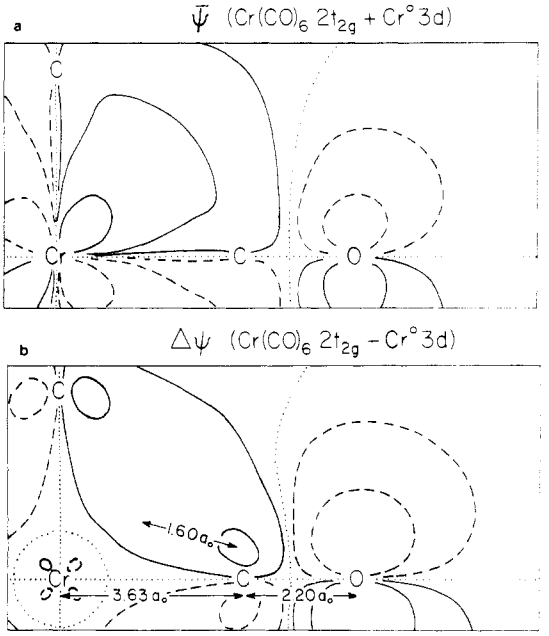

Figure 6. (a) $^1/_2[\psi(\vec{r})_{2t_{2g}} + \psi(\vec{r})_{Cr\,3d}]$. (b) $\psi(\vec{r})_{2t_{2g}} - \psi(\vec{r})_{Cr\,3d}$.

the $B(r)$ functions obtained from the HF wave functions at Cr–C distances of 1.92 and 2.06 Å and from the experimental data (peak A). For both the equilibrium distance HF calculation and experiment, we find a maximum in $\Delta B(r)$ (defined as $B(r)$ for the molecular orbital minus $B(r)$ for the Cr 3d atomic orbital) around 1.6–1.8 a_0 and a minimum around 3.6–4.4 a_0. For the elongated Cr–C bond, the $\Delta B(r)$ function is flatter and everywhere negative. Although our approximate method of normalizing calculated and experimental $\rho(q)$'s certainly introduces some uncertainty, it appears that the $2t_{2g}$ orbital in the elongated geometry is more like the free atom Cr 3d orbital, as would be expected. Indeed, the HF calculation of Sherwood and Hall[23] indicates that an increase in the Cr–C distance of 0.25 Å greatly reduces the Cr 3d–CO 2π back-bonding interaction. Given the increase of 0.14 Å in Cr–C distance estimated for the $2t_{2g}$ $Cr(CO)_6^+$ cation,[20] it seems that the most appropriate Cr–C distance for comparison with the experimental $\rho(q)$ should be somewhat larger than 1.92 Å (see ref 27). This increase in the Cr–C distance would probably result in somewhat better agreement of the calculated and experimental $\Delta B(r)$'s. However, the effect of correlation, which would tend to increase Cr 3d–CO 2π bonding,[23] should also be taken into account. Finally, we should note that the $q^2\rho(q)$ distributions for the free Cr atom and for the $Cr(CO)_6$ $2t_{2g}$ MO at equilibrium and expanded Cr–C distances differ most in the region above 1.5 $\hbar a_0^{-1}$, where the experimental data are least accurate.

A simple interpretation of the $\Delta B(r)$ function for equilibrium $Cr(CO)_6$ may be obtained by plotting the average and difference of the $Cr(CO)_6$ $2t_{2g}$ and free atom Cr 3d orbital amplitudes shown in Figure 6. The ψ map (Figure 6a) looks qualitatively like ψ for the $2t_{2g}$ MO but with the CO 2π contribution reduced. The $\Delta\psi$ plot accentuates the CO 2π contributions to the $2t_{2g}$ orbital. We have found for the CO, NO, and O_2 series[25] and for NH_3 and CH_3NH_2[13] that extrema in $\Delta B(r)$ can often be identified with maximums and minimums in $\bar{\psi}$ and $\Delta\psi$. The extrema in the $\bar{\psi}$ plot are the Cr 3d orbital lobes while the extrema in the $\Delta\psi$ plot are the p-orbital lobes on C and O. In the $\Delta\psi$ plot (Figure 6b) we have drawn a vector of length 1.6 a_0 from the C 2p lobe toward the Cr 3d lobe. Qualitatively, the maximum in $\Delta B(r)$ around 1.6 a_0 is associated with the separation of these two features. The minimum in $\Delta B(r)$ around 3.8 a_0 is then associated with a vector from the Cr 3d orbital maximum in $\bar{\psi}$ to the O 2p orbital minimum (above the Cr–C–O vector) in $\Delta\psi$. The separation of the maximum and minimum in $\Delta B(r)$ is 2.2 a_0, virtually identical with the C–O distance. Thus, the $\Delta B(r)$ plot can be interpreted in terms of a bonding interaction of a predominantly Cr 3d orbital with a CO π^* orbital, in agreement with the qualitative picture.

Conclusions

Our results confirm the previous assignments of the PES; i.e., the lowest BE corresponds to the $2t_{2g}$ MO, the BE's from 13.4 to 16.2 eV correspond to predominantly CO 5σ and 1π orbitals, and the BE near 17.8 eV corresponds to CO 4σ type orbitals. The best match between the experimental momentum densities and those obtained by synthesis of HFS orbital momentum densities is obtained if we assume that the $8a_{1g}$ orbital has a binding energy of about 16 eV. The large value of $\rho(q)$ at $q = 0$ for the 17.8-eV peak indicates both that the $8a_{1g}$ orbital lies less than 2 eV from this energy and that the $7a_{1g}$ ionization occurs very close to 17.8 eV. This is consistent with the localized-hole HFS[9a] calculations for this state and with MS–Xα[10a] calculations (for delocalized cationic states). The presence of significant CO 5σ character in the $7a_{1g}$ MO is also confirmed. Since the $7a_{1g}$ ionization occurs around 17.8 eV, the peak at 19.7 eV in the PES must be assigned as a satellite. The momentum densities measured for peaks at 20.7 and 23.5 eV indicate that they are satellites of primary peaks around 15.5 and 17.8 eV. The satellite separation energy of about 5 eV suggests a Cr 3d → CO 2π excitation as the source of these satellites.

Fourier transformation of the $2t_{2g}$ orbital momentum density and that for the free atom Cr3d orbital yield a $\Delta B(r)$ function that can be interpreted in terms of Cr 3d–CO 2π mixing. The magnitude of this mixing cannot presently be determined accurately due to various experimental and interpretational uncertainties. Nonetheless, the qualitative evidence for Cr 3d–CO 2π mixing is clear.

Acknowledgment. This work was supported by the National Science Foundation under Grant No. CHE-8205884, by the Computer Science Center, University of Maryland, and by the Netherlands Organization for Chemical Research (SON) with financial aid from the Netherlands Organization for the Advancement of Pure Research (ZWO).

Appendix

The Slater type orbital basis used in the HFS calculation consisted of the following functions and exponents:

Cr		C		O	
1s	18.70	1s	5.40	1s	7.36
2s	8.45	2s	1.24	2s	1.70
2p	9.90	2s′	1.98	2s′	2.82
3s	3.25	2p	0.96	2p	1.30
3s′	5.00	2p′	2.20	2p′	3.06
3p	2.85				
3p′	4.65				
3d	1.24				
3d′	2.70				
3d″	5.70				
4s	1.00				
4s′	1.75				
4p	2.00				

Registry No. $Cr(CO)_6$, 13007-92-6.

(27) Levin, V. G.; Neudatchin, V. G.; Pavitchenkov, A. V.; Smirnov, V. F. *J. Chem. Phys.* **1975**, *63*, 1541.
(28) Rozendaal, A.; Baerends, E. J., unpublished results.
(29) Baerends, E. J., personal communication.